(Received 6 November 2024, Accepted 17 February 2025, Scheduled 24 February 2025)

Design and Fabrication of SRR Loaded Cantor Fractal Slotted DGS Antenna Using Quarter Wave Transformer Fed for Microwave C-Band Communication

Anuj K. Sharma*, Vipul Sharma, and Sanjay Singh

Department of Electronics & Communication Engineering, Gurukul Kangri Deemed to be University Haridwar 249401, Uttarakhand, India

ABSTRACT: The design, fabrication, and measurement of a 70 mm × 60 mm × 1.6 mm high-bandwidth Cantor fractal slotted defected ground surface (DGS) antenna for the microwave C-band (4–8 GHz) are presented in this study. This multiband antenna has the best performance ever because it combines a Cantor-inverted Cantor fractal slot with a microstrip quarter-wave transformer feeding network. With simulated operating bands spanning 3.37–3.48 GHz, 4.22–5.67 GHz, and 6.74–8.25 GHz, this antenna demonstrates exceptional simulated impedance bandwidths of 110 MHz, 1.43 GHz, and 1.51 GHz with simulated reflection coefficients of −27.22 dB, −28.23 dB, and −14.71 dB at resonance frequencies of 3.44 GHz, 5.03 GHz, and 7.17 GHz, respectively. Furthermore, the antenna exhibits simulated high gains of 5.6 dB, at 5.03 GHz resonating frequency. The introduction of a split ring resonator (SRR) at the ground surface unlocks the complete simulated bandwidth of 4.13–8.14 GHz and boosts the simulated gain to 6.1 dB. The design of this SRR at 5.03 GHz shifts one band from 3.44 GHz to 2.97 GHz with a simulated bandwidth of 60 MHz. The VSWR value of this design is very close to 1. Consequently, its good impedance matching enhances the antenna's wideband performance. This is beneficial because patch antennas usually have a limited bandwidth. In addition, the antenna simulation displays an exactly symmetrical radiation pattern with current densities of 268 A/m and 155 A/m at 5.03 GHz with and without SRR, respectively.

1. INTRODUCTION

1.1. Introduction to Fractals and Antennas

The concept of fractals was first introduced by Mandelbrot [1], a pioneer in fractal geometry. The term "fractal" originates from the Latin word "fractus" meaning irregular or broken. Fractals have unique properties that make them ideal for antenna design [2]. Antennas are categorized based on their bandwidth: narrowband ($<$ 500 MHz), wideband ($>$ 500 MHz), ultra-wideband (UWB), and super wideband.

1.2. Classification and Applications of Antennas

Narrowband antennas have limited applications in wireless communications due to their low bandwidth. In contrast, wideband antennas operate at frequencies exceeding 500 MHz and have numerous applications in wireless communications. UWB antennas, designed to span both narrowband and wideband frequencies, operate from 3.1 to 10.6 GHz, as allocated by the Federal Communications Commission (FCC) [2, 3].

1.3. Fractal Antennas and Research Gap

Fractal antennas have gained popularity due to their compact size, low weight, and multi-band capacity [4]. However, existing fractal antenna designs often result in multi-narrowband responses rather than true UWB performance. Recent studies have explored the use of fractal curves, such as Koch and Minkowski curves, to improve antenna performance [11–21]. This research aims to address the knowledge gap in existing fractal antenna designs.

1.4. Key Findings of Previous Work

Previous studies have reported the following key findings:

- Fractal antennas can achieve compact size and multi-band capacity [4].
- Slot loading can introduce notch bands in UWB antennas. Due to this, the UWB system becomes interfered by nearby narrowband wireless applications such as WLAN (5.15–5.82 GHz), X-band (7.25–8.39 GHz), C band (3.8–4.2 GHz), and Wi-MAX (3.3–3.6 GHz) [5–9].
- Sharma et al. discuss how antenna array improves the total gain of the antenna. The authors also discuss the effect of mutual coupling on the total gain [10].
- On a Rogers RT Duroid 5880 substrate, Abdelaziz and Hamad have constructed a small, inset-fed, tri-band dual symmetrically separated inverted T-slotted antenna. A peak gain of 11.72 dBi is demonstrated by the antenna at 38 GHz for millimeter-wave applications and 5G services [11].

* Corresponding author: Anuj Kumar Sharma (anujsharma@gkv.ac.in).

- A dual-polarization, slotted, coaxially fed dual wideband antenna has been demonstrated by Liu et al. There are two concentric slots. The rectangular patch's center has one U-slot and one fractional U-slot. This antenna offers a peak gain of 8.6 dBi at a frequency of 5.2 GHz [12].
- An inset-fed rectangular circular slotted antenna for quad-band operation was presented by Kaur and Sharma on an FR-4 substrate. At 8.72 GHz, the antenna demonstrates a peak gain of 11.45 dBi. Applications in the S-band, C-band, and X-band are appropriate for the proposed antenna [13].
- Printed Inverted-F antennas with dual-band, dual-sense circular polarization, and 3 dB-axial ratios for the 2.5 GHz band (5.5% fractional bandwidth) and 3.5 GHz band (10.0% bandwidth) have been proposed, studied, and discussed by Shimizu and Fujimoto [14].
- An antenna that can be reconfigured for the use in both narrowband and wideband frequencies was created by Varshney et al. [15] using a PIN diode (BAR6402V).
- A high-gain complementary split-ring resonator (CSRR) loaded multiband rectangular patch antenna array was discussed by Sharma et al. [16].
- A novel approach to wireless data transmission makes use of short-pulse, low-powered radio signals to transmit enormous amounts of digital data across a broad frequency spectrum. UWB signals and systems have bandwidths larger than 500 MHz or a relative bandwidth (BW) higher than 20%.
- Multiple input multiple output antenna communication with implementation challenges was discussed by Sharma et al. [17].
- A study by Varshney et al. [18] looks at how MIMO antennas are used. Recent years have witnessed considerable interest in the construction of tiny and easily integrated MIMO antennas. This is due to the capability of these antennas to be utilized in communication technologies necessitating different frequencies and functionalities.
- Sharma et al. [19] discuss the role of fractals in the miniaturization of antenna design at the 2.4 GHz ISM band.

1.5. Motivation of Research

Previous studies have explored the use of fractal curves in antenna design to achieve compact size and multi-band capacity. For instance, Fonseca et al. designed an antenna with a single-unit Koch curve that exhibits vertical symmetry and is in its third iteration [20]. This design produces quad-narrow bands with a peak gain of 5.71 dBi at 2.37 GHz. However, this design has limited bandwidth. Sharma and Sharma [21] proposed two distinct antenna designs that improve upon the limitations of Fonseca et al.'s design. The first design incorporates two units of Koch-Koch curves in the middle of the antenna patch, along its width. The second design uses a hybrid combination of one unit of Koch and one unit of Minkowski curves in the middle of the patch, along its width. While these designs demonstrate improved performance, they still fall short of achieving true UWB performance. The research gap in existing fractal antenna designs motivates our work. Specifically, we aim to create a novel fractal shape that achieves UWB performance, rather than multi-narrowbands. To address this challenge, we propose a new approach that combines two units of cantor fractal curves placed oppositely. This design is expected to exhibit improved bandwidth and gain, making it suitable for UWB applications.

1.6. Research Objectives

The primary objective of this research is to design a novel fractal slotted antenna geometry using two units of Cantor fractal curves placed oppositely, achieving UWB performance. Another objective is to investigate the effect of SRR on the proposed antenna's performance.

1.7. Organization of the Paper

The paper is organized as follows. Section 2 describes the material and method. Section 3 gives an overview of the studied parameters. Section 4 presents simulated and measured results, and Section 5 concludes the research.

2. MATERIAL AND METHODS

2.1. Process of Proposed Antenna Design with Cantor-Inverted Cantor Fractal Curve

Figure 1 shows a small ultra-wideband (UWB) antenna with fractal slots. It is built on a thin 1.6 mm FR-4 substrate that has a relative permittivity of 4.4 and a loss tangent of $\tan\varepsilon = 0.02$.

FR-4 substrate is commonly utilized for frequencies below 10 GHz [25]. We can use this low-cost substrate for antenna designs at frequencies below 10 GHz. Here, we use an ANSYS Electronic Desktop Terminal (EDT), specifically High Frequency Structure Simulator (HFSS), to analyze and compute the suggested antenna design. The proposed antenna has been specifically engineered to operate at a frequency of 5.03 GHz. The dimensions of the microstrip square substrate and ground were initially determined to be 70 mm in width and 70 mm in length at the specified design frequency. To enhance the resulting performance characteristics, the values have been adjusted to a rectangular substrate of 70 mm in length and 60 mm in width as shown in Table 1. A quarter-wave transformer with a length of 13.2 mm and a width of 0.75 mm was employed to achieve perfect impedance matching with a 50 Ω center-fed transmission line. The transmission line itself had a width of 3.05 mm and a length of 4.1 mm. Next, a Cantor fractal and an inverted cantor fractal with a width of 27 mm and length of 0.8 mm are presented. Afterward, the ideal length of the ground was found using the optimization tool of HFSS, resulting in an optimized length of 15 mm for DGS. This allows us to attain one narrowband and two widebands, namely ranging from 3.37 to 3.48 GHz, 4.22 to 5.67 GHz, and 6.74 to 8.25 GHz. By integrating a split ring resonator (SRR) at the ground with precise dimensions (outer radius $(R_{out}) = 3.6$ mm, width $(W) = 0.95$ mm, gap $(S) = 0.7$ mm), it was possible to achieve a

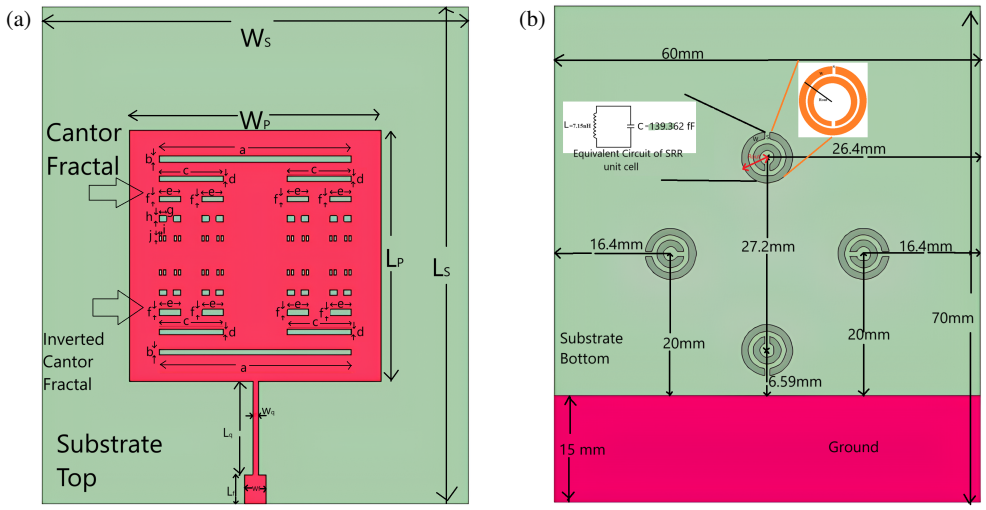

FIGURE 1. (a) Front view. (b) Bottom view.

TABLE 1. Proposed antenna's variables.

Variable	Dimension (mm)
L_s	70
W_s	60
W_p	35.4
L_p	35.4
W_q	0.75
L_q	13.2
W_g	60
L_g	70
W_f	3.05
L_f	4.1
A	27
B	0.8
C	9
D	0.8
E	9
F	0.8
G	3
H	0.8
I	0.33
J	0.8
R_{out}	3.6
W	0.95
S	0.7

UWB frequency range that spans from 4.13 to 8.14 GHz and has a gain of 6.1 decibels.

2.2. Split Ring Resonator (SRR) Design

Placing an SRR on the ground plane with specific dimensions, as illustrated in Fig. 1(b), will affect both the bandwidth and the total gain of the antenna when the patch and ground sizes remain intact. Fig. 1(b) also depicts the equivalent circuit values of inductance $(L) = 7.15$ nH and capacitance $(C) = 139.362$ fF at 5.03 GHz.

Table 1 illustrates the numerical values of variables shown in Fig. 1.

2.3. Antenna Fabrication and Measurement

The antenna, created along with optimum dimensions by photolithography, UV exposure, and chemical etching, is produced on a 1.6 mm thick flame retardant-4 epoxy substrate shown in Figs. 2(a), 2(b), 2(c), and 2(d). The constructed antenna undergoes testing for S_{11} validation using the Agilent N5247A VNA and radiation pattern validation on an anechoic chamber shown in Figs. 2(e), 2(f), and 2(g), 2(h), respectively.

3. MATHEMATICAL CALCULATIONS

The following parameters are used for the proposed antenna's variable calculation.

$$\text{Permittivity } (\varepsilon_r) = 4.4 \text{ for FR-4}$$
$$\text{Dielectric Height } (h) = 1.6 \text{ mm}$$

3.1. Patch's Calculation

Figure 3 illustrates the preliminary design of the proposed antenna with quarter-wave transformer feed, and the length (L_p) can be determined using Equations (1) and (2) [22].

$$L_P = \frac{F}{\left\lfloor 1 + \frac{2h}{\pi\varepsilon_r F}\left\lceil \ln\left(\frac{\pi F}{2h}\right) + 1.7726\right\rceil\right\rfloor^{1/2}} \times 2 \quad (1)$$

were

$$F = \frac{8.79X10^9}{f_r\sqrt{\varepsilon_r}} \quad (2)$$

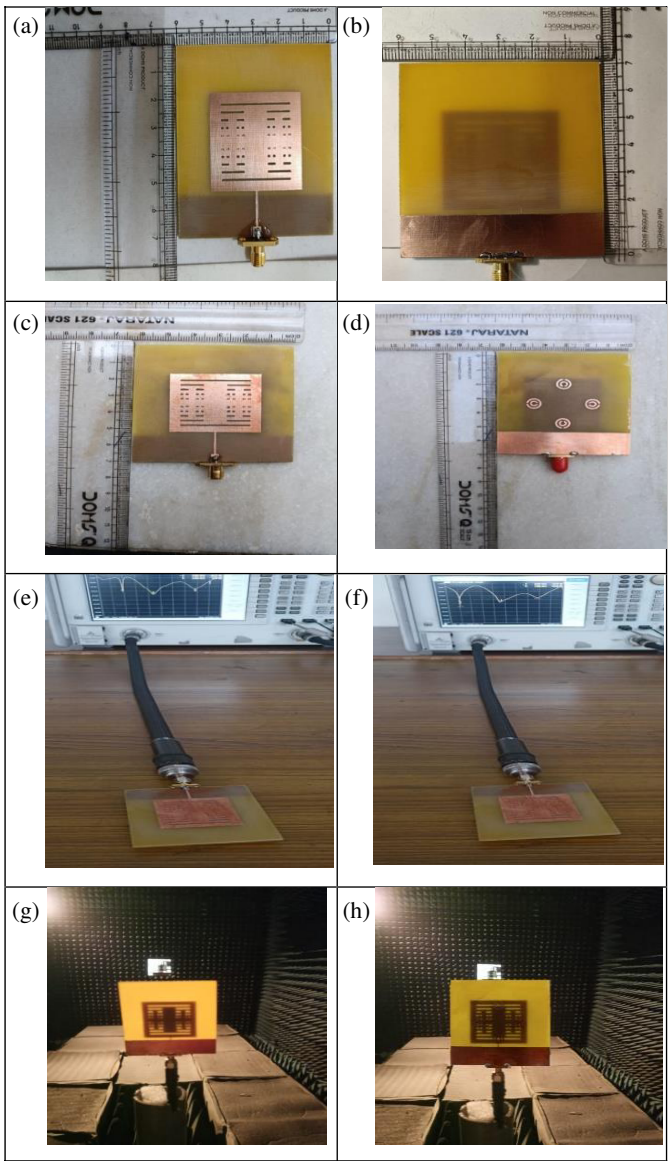

FIGURE 2. (a) Fabricated (Top) without SRR. (b) Fabricated (Back) without SRR. (c) Fabricated (Top) with SRR. (d) Fabricated (Back) with SRR. (e) S_{11} Measurement using VNA Agilent N5247A of proposed antenna without SRR. (f) S_{11} Measurement using VNA Agilent N5247A of proposed antenna with SRR. (g) Measurement of radiation in anechoic chamber of proposed antenna without SRR. (h) Measurement of radiation in anechoic chamber of proposed antenna with SRR.

3.2. Quarter Wave Transformer Calculation

$$\begin{aligned} Zc &= \sqrt{ZoZL} \\ &= \sqrt{50X243} \\ &= \sqrt{12150\,\text{mm}} \\ &= 110.22\,\text{mm} \end{aligned}$$

Feeder width (W_f) is calculated by (3) and (4) [21].

$$W/h = \frac{8e^A}{e^{2A}-2} \tag{3}$$

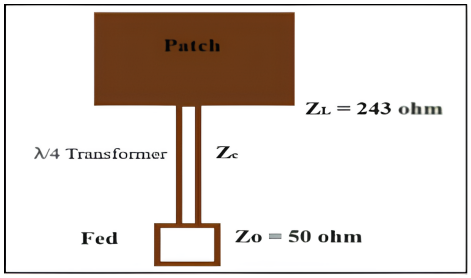

FIGURE 3. Quarter-wave transformer fed.

$$\text{where } A = \frac{Zc}{60}\left(\frac{\varepsilon_r+1}{2}\right)^{1/2} + \frac{\varepsilon_r-1}{\varepsilon_r+1}\left(0.023+\frac{0.11}{\varepsilon_r}\right) \tag{4}$$

3.3. Effect of Defected Ground on Proposed Antenna

A Defected Ground Surface (DGS) is a technique used in antenna design to improve its performance by etching a specific pattern or shape on the ground plane. Some advantages of DGS are improved impedance matching, increased bandwidth, enhanced gain, reduced size, and improved isolation [27]. When a ground conductor covers the whole bottom surface of the substrate, and a Cantor-inverted Cantor fractal slot is etched into the top surface of a rectangular patch, the resulting slotted microstrip antenna acts as a multi-tuned narrow-band antenna. When the ground plane is reduced close to the feed without altering its width, the antenna transforms into a wide-band antenna.

4. OUTCOMES AND CONVERSATIONS

4.1. Reflection Coefficient vs Frequency

Reflection coefficient is a measure of how much power is reflected back at an interface between two transmission lines or media, rather than being transmitted forward. A reflection coefficient of -10 dB or lower indicates that only a small fraction of the power is reflected, while most is transmitted [28]. The antenna, fabricated along with optimum dimensions, is shown in Figs. 2(a), 2(b), 2(c), and 2(d). The simulated S_{11} plot, which can be seen in Figs. 4(a) and 4(b), has resonance frequencies of 3.44 GHz (without SRR), 2.97 GHz (with SRR), 5.03 GHz (with or without SRR), 7.17 GHz (without SRR), and 7.19 (with SRR) with reflection coefficients of -27.22 dB, -35.82 dB, -28.23 dB, -29.64 dB, -14.71 dB, and -15.85 dB, respectively. The constructed antenna undergoes testing for S_{11} validation using the Agilent N5247A VNA. The measured reflection coefficient S_{11} exhibits a fractional bandwidth (FBW) of 78.2% throughout a measured range of frequencies from 4.14 GHz to 8.13 GHz with SRR on the ground surface. The simulated FBW of the proposed antenna with SRR on ground (4.13–8.14 GHz) is almost 0.015% larger than the measured FBW of the proposed antenna with SRR on ground (4.14–8.13 GHz), as detailed in Fig. 4(d). According to Figs. 4(c) and 4(d), it is pretty obvious that the simulated and those that measured values are slightly different. This is because of the soldering effect that occurs during the fabrication process.

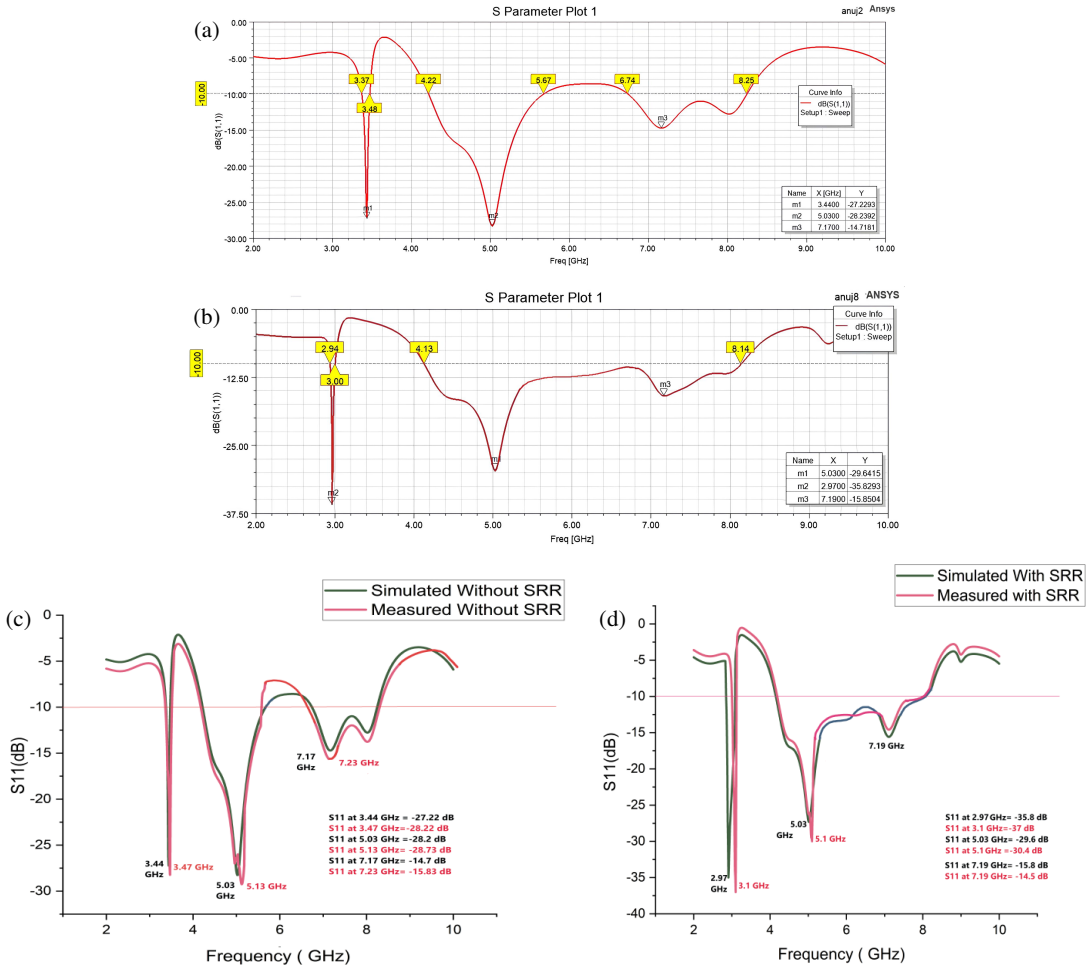

FIGURE 4. (a) S_{11} plot (Simulation done on 5.03 GHz Frequency using HFSS) without SRR. (b) S_{11} plot (Simulation done on 5.03 GHz frequency using HFSS) with SRR. (c) Simulated and measured S_{11} plots on 5.03 GHz without SRR. (d) Simulated and measured S_{11} plots on 5.03 GHz with SRR.

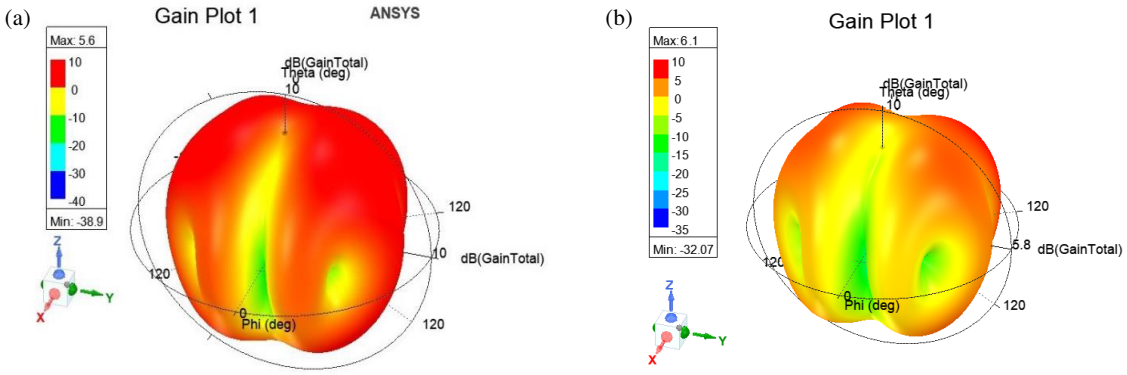

FIGURE 5. (a) Gain at 5.03 GHz without SRR. (b) Gain at 5.03 GHz with SRR.

4.2. Gain Plot

In the context of antennas, a gain plot represents the directional dependence of an antenna's gain. It is a graphical representation of how the antenna's gain varies in different directions. A gain plot for an antenna typically shows the gain (in decibels, dB) as a function of azimuth angle (θ) and elevation angle (φ). The gain plot is shown in Figs. 5(a), and 5(b) shows that the maximum gain value is 5.6 dB at 5.03 GHz when the SRR is not introduced at the ground and 6.1 dB at the same frequency when the SRR is introduced at the ground.

4.3. Field Plot

The E plot facilitates the visualization of the antenna's emission pattern, illustrating the direction and intensity of the electric

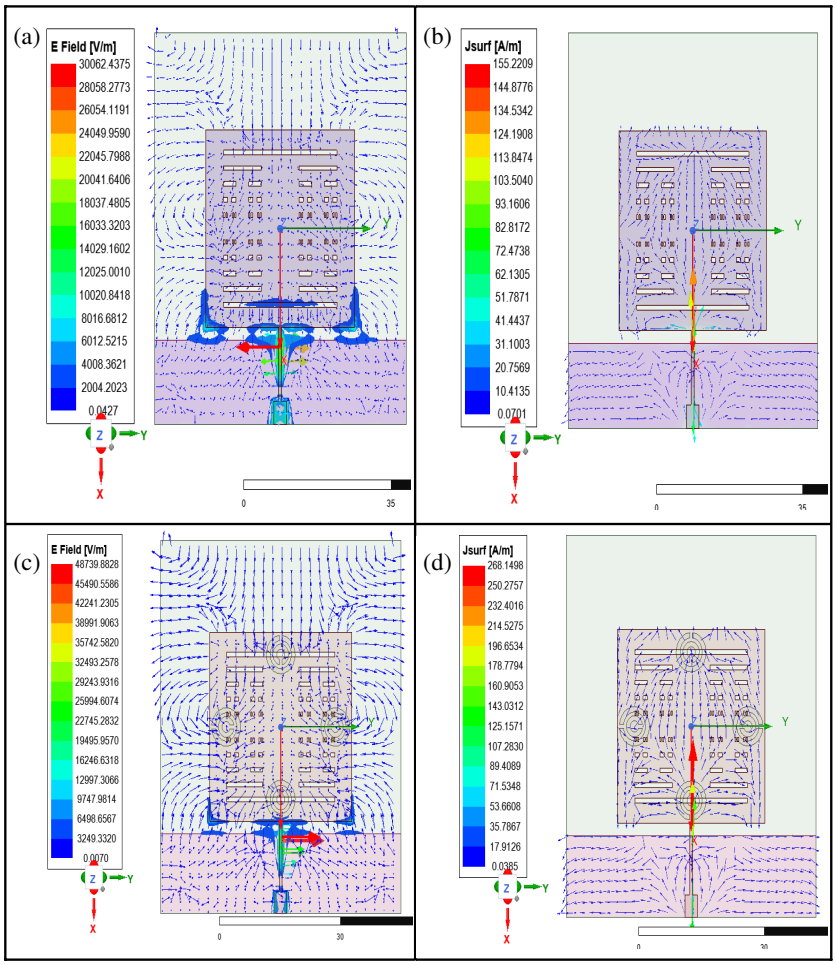

FIGURE 6. (a) E-field (V/m) at 5.03 GHz without SRR. (b) Jsurface at 5.03 GHz without SRR. (c) E-field (V/m) at 5.03 GHz with SRR. (d) Jsurface at 5.03 GHz with SRR.

field. These plots also explain the intensity of the electric field at various locations surrounding the antenna.

The J plot illustrates the current distribution on the antenna, aiding engineers in comprehending the excitation of the antenna. The J plot can also reveal regions of elevated current density, potentially resulting in heightened losses and diminished antenna efficiency. Here, Figs. 6(a), 6(b), 6(c), and 6(d) show the E-field and J-field plot at resonance frequency.

4.4. Gain Vs Frequency Plot

The gain vs frequency plot is a graphical representation of an antenna's gain (directivity) as a function of frequency. This plot provides valuable insights into an antenna's performance across different frequencies. The y-axis represents the antenna's gain, typically measured in decibels relative to isotropic (dBi).

The x-axis represents the frequency range over which the antenna's gain is measured. The frequency at which the antenna's gain is maximum is called the resonance frequency. The plot helps determine if the antenna is tuned to the desired frequency. A peak in the gain at the desired frequency indicates proper tuning. The plot reveals the antenna's bandwidth, which is essential for applications requiring operation over a range of frequencies. The gain vs frequency plot can also provide insights into the antenna's efficiency, as a higher gain typically indicates higher efficiency. Here in Fig. 7, the gain remains almost constant between 4.13 GHz and 8.14 GHz, and the peak gain is 8.25 dBi (Simulated with SRR), 8.15 dBi (Measured with SRR), 7.75 dBi (Simulated without SRR), and 7.45 dBi (Measured without SRR) at its resonance frequency 5.03 GHz.

4.5. Radiation Pattern Plot

A radiation pattern plot is a graphical representation of an antenna's radiation properties, showing how the antenna radiates energy in different directions. It is a crucial tool for understanding an antenna's performance and behavior. The E-plane is defined as the plane that contains the electric field vector (E) and the direction of maximum radiation. For a linearly polarized antenna, the E-plane is typically aligned with the antenna's electric field vector. When Phi $= 90$, the E-plane is aligned with the x-axis (or the horizontal plane), which means that the electric field vector is parallel to the x-axis [27]. The H-plane is defined as the plane that contains the magnetic field vector (H) and is perpendicular to the E-plane. For a linearly polarized an-

TABLE 2. Simulated and measured results of the proposed antenna.

Antenna	Res. Freq., f_r (GHz)	Ref. Coeff, S_{11} [dB]	BW (GHz)	FBW (%)	VSWR	Gain (dB)
Simulated Without SRR	3.44/ 5.03/ 7.17	−27.22/ −28.23/ −14.71	3.37–3.48 4.22–5.67 6.74–8.25	3.19 28.8 21.05	1.04 @5.03 GHz	5.6 @5.03 GHz
Simulated With SRR	2.97/ 5.03/ 7.19	−35.82/ −29.64 −15.85	2.94–3 4.13–8.14	2.02 79.7	1.02 @5.03 GHz	6.1 @5.03 GHz
Measured Without SRR	3.47/ 5.13/ 7.17	−28.22/ −28.73/ −15.83	3.36–3.44 4.2–5.64 6.71–8.3	2.3/ 27.1/ 22.1	1.10 @5.03 GHz	5.6 @5.03 GHz
Measured With SRR	3.1/ 5.1/ 7.19	−37/ −30.4/ −14.5	2.98–3.2/ 4.14–8.13	7.09/ 78.2	1.11 @5.03 GHz	6.1 @5.03 GHz

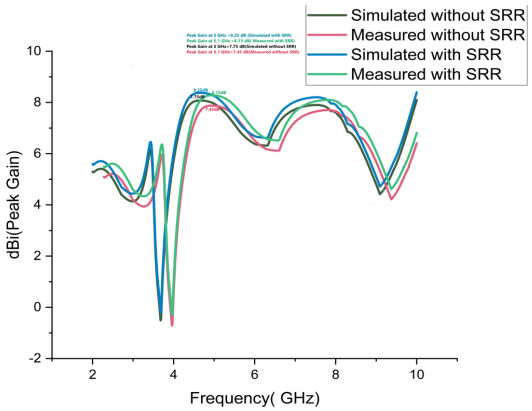

FIGURE 7. Gain vs frequency.

tenna, the H-plane is typically aligned with the antenna's magnetic field vector. When Phi $= 0$, the H-plane is aligned with the y-axis (or the vertical plane), which means that the magnetic field vector is parallel to the y-axis [27]. The simulated and measured radiation plots in E-plane and H-plane are displayed in Figs. 8(a) and 8(b). All simulation is carried out in HFSS, and a comparison plot between the simulated and measured values is plotted in software Origin.

Table 2 demonstrates the comparison between the simulated and measured results of the proposed antenna, which indicates that the disparity between simulated and measured results is minimal.

4.6. Performance Comparison of the Proposed Antenna with Similar Existing Antennas

Sharma and Sharma proposed the use of single Koch-Koch and Minkowski-Minkowski fractal slots to construct two rectangular patch antennas, each measuring 45 mm × 38.92 mm. One of the antennas was narrowband, while the other was wideband [21]. Antennas with fractal slots have been designed and developed for multi-band applications using a variety of different shapes and sizes of arms, including fan-shaped, circular, Mickey-Mouse ear-shaped, log-periodic nine square fractal slots, double U-shaped, double T-shaped, and double Koch slot fractals [11, 12, 15, 21, 23]. The proposed antenna does better than others in every way. It has a UWB bandwidth of 4.13 GHz–8.14 GHz, a frequency that is triple-tuned, and a small size of 70 mm × 60 mm. With a quarter-wave transformer-fed and Cantor-inverted Cantor fractal slot, an overall simulated FBW of 79.7% has been reached compared to the base antenna [21]. Table 3 shows a comparison of the suggested antenna's performance parameters with those of similar antennas that already exist.

4.7. Proposed Antenna's Originality in Relation to the Reference Antenna [21]

The suggested antenna presents multiple improvements compared to the reference design antenna [21].

The suggested antenna and reference antenna were both designed for a frequency of 5.03 GHz; however, the proposed design achieved a simulated FBW of 79.7%. The proposed antenna design exhibits multiband application, a minimum reflection coefficient of −29.64 dB, and improved voltage standing wave ratio (VSWR) concerning the reference antenna [21]. The advancement of the suggested antenna prototype compared to the reference antenna is illustrated in Table 4.

Table 3 demonstrates that the suggested antenna outperforms the antennas documented in the current literature in almost all respects. The suggested antenna uses a new, mutually coupled feed that has not been used in antenna arrays before to make sure that the patch and feeding network have the best impedance matching. In this way, the antenna gets both high gain and bandwidth at the same time. The literature suggests that no one has previously utilized the Cantor-inverted Cantor fractal on the patch. Table 4 explains how the proposed antenna outperforms the reference antenna in terms of gain and bandwidth at the same time [21]. S_{11} is also improved in the proposed antenna.

TABLE 3. Performance comparison of the proposed antenna with existing literature.

Ref.	Substrate (Feeding type)	Resultant Fractal Slot	Size (mm^2)	Res. Freq. (GHz)	−10 dB BW	FBW (%)	Gain (dBi)
[24] 2015	Roger RO4003 $\varepsilon_r = 3.55$ $h = (1.524 + 1.524)$ mm $\tan\delta = 0.0021$ (Proximity fed)	9-Square fractal Log-Periodic	173×70	3.2/3.6, 3.95/4.2, 4.55, 5.0/ 5.5/6.52/ 7.2, 7.8, 8.3, 10.2, 10.9	3.1–3.3 3.5–4.1 4.2–5.1 5.2–5.8 6.2–6.75 6.9–11.0	6.25 15.78 19.35 10.9 8.5 45.81	11.15 @5 GHz
[11] 2019	Rogers RT Duroid 5880 substrate $\varepsilon_r = 2.2$, $\tan\delta = 0.0009$ $h = 0.508$ mm (Inset fed)	Double Separate T-Shaped Slots	20×16.5	10/28/38	9–11 27–29 37–39	20 7.14 5.26	5.82 11.48 11.72
[12] 2013	(Coaxial fed)	Double U-shaped slots	50×50	3.6/5.2	3.49–3.74 4.92–5.42	7.5 9.6	8.5 8.6
[13] 2017	FR-4 $\varepsilon_r = 4.4$ $h = 1.6$ mm $\tan\delta = 0.02$ (Inset fed)	5 Rectangule+ 5 Circule slots	55×35.5	2.81/5.81/7.81, 8.0/8.72	2.79–2.98 5.68–5.9 7.65–8.2 8.6–9.0	1.4/ 1.5/ 1.3, 1.2/ 1.2	3.22/ 4.68/ 5.94, 8.09/ 11.45
[15] 2021	Rogers RT Duroid 5880 substrate $\varepsilon_r = 2.2$, $\tan\delta = 0.0009$ $h = 1.57$ mm (Edge fed)	Ear shaped circular	40×45	7.4, 11.8, 17.2, 20.2, 24.8, 30.3, 38.6	1.22–47.5	190	Varies between 0.2 to 9.7
[23] 2021	FR-4 $\varepsilon_r = 4.4$ $h = 1.6$ mm $\tan\delta = 0.02$ (Edge fed)	Tri-Rectangular Arms fractals	66.4×66.4	2.45	1.81–3.0	48.98	7.16
[20] 2019	FR-4 $h = 1.5$ mm $f_0 = 2.4$ GHz $\tan\delta = 0.02$ (Inset Fed)	Double separate Koch slots	37.29×29.06	2.4/4.48/7.57, 8.0/9.4	2.3–2.45 4.4–4.6 7.3–8.1 9.2–9.7	6.25 4.46 10.38 5.31	5.71 dBi @2.37 GHz
[21] 2018	FR-4 $\varepsilon_r = 4.4$ $h = 1.6$ mm $\tan\delta = 0.02$ (Transformer fed)	Single Koch-Koch	45×38.92	2.77/8.38	2.51–2.90 7.74–10	14.07 26.96	3.72/7.77
	FR-4 $\varepsilon_r = 4.4$ $h = 1.6$ mm (Transformer fed)	Single Koch-Minkowski	45×38.92	2.46/8.34	2.38–2.58 7.56–10	8.13 29.25	5.73/5.62
[26] 2023	FR-4 $\varepsilon_r = 4.4$ $h = 1.6$ mm $\tan\delta = 0.02$ (Off-set Edge-fed)	Koch plus Minkowski hybrid fractal	38.12 mm 38.42 mm	3.2/4.94/ 7.21/10.10 GHz	2.85–11.32	119.55	6.73/5.91/ 8.26/8.02
This Work	FR-4 $\varepsilon_r = 4.4$ $h = 1.6$ mm $\tan\delta = 0.02$ (Quarter wave transformer fed)	Cantor-inverted Cantor fractal	70×60	Simulated Resonance Frequencies 3.44/5.03/7.17 (without SRR) 2.97/5.03/7.19 (with SRR)	Simulated Bandwidth 3.37–3.48/4.22–5.67/ 6.74–8.25 (without SRR) 2.94–3/4.13–8.14 (With SRR)	Simulated FBW 3.19 28.8 21.05 (without SRR) 2.02 79.7 (With SRR)	5.6 dB @5.03 GHz (without SRR) 6.1dB @5.03 GHz (With SRR)

TABLE 4. The originality of the proposed antenna with reference antenna [21].

Based on	Parameter	Reference antenna [21]	Novelty in This work	Achievements
Antenna Geometry	Feeding Technique	Quarter wave impedance transformer fed	Quarter wave impedance transformer fed	Better Impedance matching in terms of better reflection coefficient (lowest $S_{11} = -29.64$ dB)
	Fractal curves used	Single-single Hybrid fractal Curve combination of Koch-Minkowski	Cantor-inverted cantor fractal (combination of Cantor fractal and inverted Cantor fractal)	More Advance Curve
	Ground	Complete ground	Partial ground with SRR	Reduced Ground size
Result Performance	Minimum Reflection Coefficient, S_{11} (dB)	-18 dB	-29.64 dB	S_{11} has been improved
	FBW	14.7% (2.41–2.82), 29.26% (7.56–10)	79.7% (4.13–8.14) With SRR	Enhanced BW
	Application Covered/Resonance Frequencies (GHz)	Dual tuned (2.79 and 8.34 (6.67–10))	Triple tuned (3.44/5.03/ 7.17 without SRR) Triple tuned (2.97/5.03/ 7.19 with SRR) (4.13–8.14)	More number of applications covered
	No. of the Frequency band	Dual (One narrowband and one wideband)	Tri (one narrowband and two Ultra-wideband) without SRR Dual (one narrowband and one Ultra-Wideband) with SRR	UWB concerning NB and WB
	Peak Antenna Gain (dB)	5.73/5.62	6.1 (With SRR)	0.37 dB antenna gain Enhancement
	Radiation pattern	Bidirectional (with a lower Front to back ratio)	Bidirectional (with better Front to back ratio)	One-sided antenna gain improved

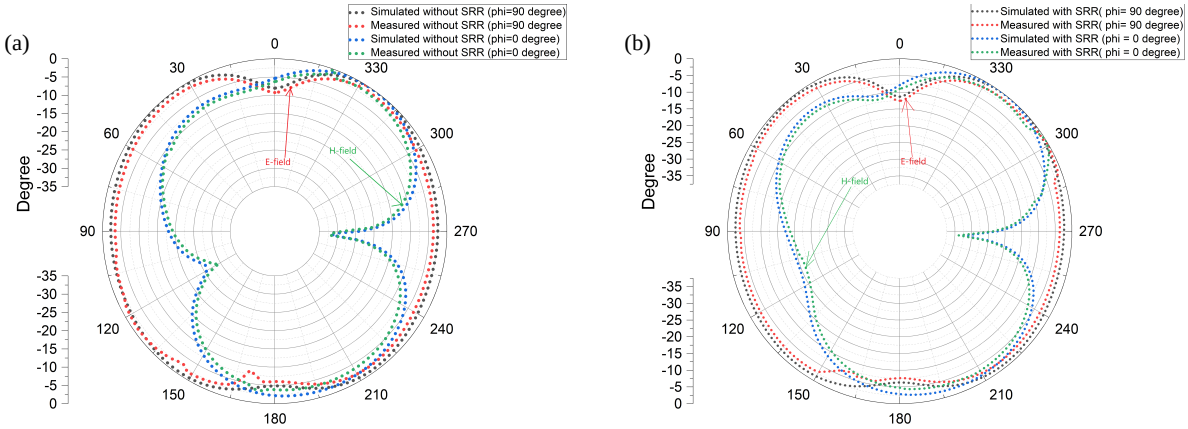

FIGURE 8. (a) Radiation pattern at 5.03 GHz (E-field and H-field) without SRR. (b) Radiation pattern at 5.03 GHz (E-field and H-field) with SRR.

4.8. Application of Proposed Antenna

The 3.14 GHz and 5.03 GHz resonances align with Wi-Fi and Wireless Local Area Network (WLAN) frequency bands, making the proposed antenna applicable to indoor and outdoor wireless communication systems. The antenna's resonance at 5 GHz makes it suitable for 5G wireless communication systems, enabling high-speed data transfer, low latency, and increased connectivity. 5.03 GHz and 7.17 GHz resonances can be utilized in air traffic control radar systems, providing accurate surveillance and tracking capabilities. The 7.17 GHz resonance is close to the frequency band used in weather radar systems, making the antenna suitable for weather monitoring and forecasting applications. 3.44 GHz and 7.17 GHz fall within the C-band and X-band frequency ranges, respectively, which are used in satellite communication systems for various applications, including telecommunications, navigation, and remote sensing. The antenna's resonances at 5.03 GHz and 3.44 GHz make it suitable for internet of things (IoT) devices, enabling wireless communication and connectivity for various applications, such as smart homes, industrial automation, and wearable devices. 7.17 GHz can also be utilized in medical imaging applications, such as microwave imaging and therapy.

5. CONCLUSIONS

A quarter-wave transformer-fed, ultra-wideband, Cantor fractal slotted defective ground surface (DGS) antenna for the microwave C-band (4–8 GHz) has been constructed, tested, and evaluated. The constructed antenna is cost-effective since it employs a flame retardant-4 substrate possessing specific dimensions of 70 mm $\times$ 60 mm $\times$ 1.6 mm. The measured and simulated findings exhibit concordance in shape, with minor significant variations at the three resonance frequencies. The suggested antenna exhibits a gain of 5.6 dB at 5.03 GHz. The full bandwidth of 4.13 GHz to 8.14 GHz and a gain of 6.1 dB are achieved upon the introduction of a split ring resonator (SRR) at the ground surface. The SRR is designed for 5.03 GHz, resulting in a frequency shift from 3.44 GHz to 2.97 GHz, while bandwidth decreases from 110 MHz to 60 MHz. The predicted and observed radiation patterns exhibit slight discrepancies at the tuning frequencies of 3.44 GHz, 5.03 GHz, and 7.17 GHz. The antenna constructed with an FR-4 substrate has elevated gain values when an SRR is incorporated at the ground plane. With an estimated simulated UWB fractional bandwidth of 79.2%, the proposed antenna is a good fit for many different types of networks and technologies, including WiFi, WLAN, PCS, WiMAX, Sub-6 GHz, radar, military, space research, satellite-fixed mobile, and C-band. It is possible to modify the suggested antenna in the future so that it may change its frequency, polarization, and pattern using varactor diodes. The suggested antenna's small size makes it suitable for the use in array systems or multiple-input multiple-output (MIMO) systems, where it could improve data rates and diversity resolution.

CONFLICT OF INTEREST (COI) STATEMENT

The authors declare that they have no conflicts of interest regarding the publication of this paper.

HUMAN AND ANIMAL RIGHTS DECLARATION

This research did not involve any human participants or animals.

ACKNOWLEDGEMENT

The Measurements were conducted at the ECE Dept. Indian Institute of Technology (IIT), Roorkee. Which provided access to the necessary equipment and resources.

DATA AVAILABILITY STATEMENT

All data generated or analyzed during this study are included in this article.

REFERENCES

[1] Mandelbrot, B., *Fractals: Form, Chance and Dimension*, W H Freeman and Co, ISBN 0-7167-0473-0, 1977.

[2] Azim, R. and M. T. Islam, "Compact planar UWB antenna with band notch characteristics for WLAN and DSRC," *Progress In Electromagnetics Research*, Vol. 133, 391–406, 2013.

[3] Syed, A. and R. W. Aldhaheri, "A very compact and low profile UWB planar antenna with WLAN band rejection," *The Scientific World Journal*, Vol. 2016, No. 1, 3560938, 2016.

[4] Gianvittorio, J. P. and Y. Rahmat-Samii, "Fractal antennas: A novel antenna miniaturization technique, and applications," *IEEE Antennas and Propagation Magazine*, Vol. 44, No. 1, 20–36, 2002.

[5] Zhao, Y.-L., Y.-C. Jiao, G. Zhao, L. Zhang, Y. Song, and Z.-B. Wong, "Compact planar monopole UWB antenna with band-notched characteristic," *Microwave and Optical Technology Letters*, Vol. 50, No. 10, 2656–2658, 2008.

[6] Liu, H.-W., C.-H. Ku, T.-S. Wang, and C.-F. Yang, "Compact monopole antenna with band-notched characteristic for UWB applications," *IEEE Antennas and Wireless Propagation Letters*, Vol. 9, 397–400, 2010.

[7] Patil, S. and V. Rohokale, "Multiband smart fractal antenna design for converged 5G wireless networks," in *2015 International Conference on Pervasive Computing (ICPC)*, 1–5, Pune, India, 2015.

[8] Abdalla, M. A., A. A. Ibrahim, and A. Boutejdar, "Resonator switching techniques for notched ultra-wideband antenna in wireless applications," *IET Microwaves, Antennas & Propagation*, Vol. 9, No. 13, 1468–1477, 2015.

[9] Zarrabi, F. B., Z. Mansouri, N. P. Gandji, and H. Kuhestani, "Triple-notch UWB monopole antenna with fractal Koch and T-shaped stub," *AEU — International Journal of Electronics and Communications*, Vol. 70, No. 1, 64–69, 2016.

[10] Sharma, A. K., V. Sharma, and S. Singh, "Design and fabrication of mutually coupled feed based cantor fractal patch antenna array for satellite communication," *International Journal of Microwave and Optical Technology*, Vol. 20, No. 2, 78–90, 2025.

[11] Abdelaziz, A. and E. K. I. Hamad, "Design of a compact high gain microstrip patch antenna for tri-band 5G wireless communication," *Frequenz*, Vol. 73, No. 1-2, 45–52, 2018.

[12] Liu, S., S.-S. Qi, W. Wu, and D.-G. Fang, "Single-fed dual-band dual-polarized U-slot patch antenna," in *2013 IEEE MTT-S International Microwave Workshop Series on RF and Wireless Technologies for Biomedical and Healthcare Applications (IMWS-BIO)*, 1–3, Singapore, 2013.

[13] Kaur, N. and N. Sharma, "Designing of slotted microstrip patch antenna using inset cut line feed for S, C and X band applications," *International Journal of Electronics Engineering Research*, Vol. 9, No. 7, 957–969, 2017.

[14] Shimizu, K. and T. Fujimoto, "A printed inverted-F antenna for dual-band dual-sense circular polarization," in *2018 IEEE International Workshop on Electromagnetics: Applications and Student Innovation Competition (iWEM)*, 1–1, Nagoya, Japan, Aug. 2018.

[15] Varshney, A., T. M. Neebha, V. Sharma, J. G. Jency, and A. D. Andrushia, "Dodecagon-shaped frequency reconfigurable antenna practically loaded with 3-delta structures for ISM band and wireless applications," *IETE Journal of Research*, Vol. 69, No. 11, 7747–7759, 2023.

[16] Sharma, A. K., V. Sharma, and S. Singh, "Design and performance analysis of CSRR loaded high gain multiband rectangular microstrip patch antenna array (1 × 2) for IoT and wireless applications," in *2024 IEEE 3rd World Conference on Applied Intelligence and Computing (AIC)*, 1185–1191, Gwalior, India, 2024.

[17] Sharma, A. K., V. Sharma, and K. Kapoor, "Historical development of spatial modulation and massive MIMO communication system with implementation challenges: A review," *International Journal of Sensors Wireless Communications and Control*, Vol. 11, No. 2, 207–215, 2021.

[18] Varshney, A., V. Sharma, and A. K. Sharma, "RLC-equivalent circuit based stub loaded 2 × 2 MIMO antenna for wireless applications," *Microwave Review*, Vol. 29, No. 1, 44–54, 2023.

[19] Sharma, A. K., V. Sharma, and S. Singh, "A comprehensive examination of the current state of the art in fractal array antennas," *Advances in Systems Science & Applications*, Vol. 23, No. 4, 104–118, 2023.

[20] Fonseca, D., F. Pereira, and U. R. C. Vitor, "Study of patch antennas with koch curve form slots," *Journal of Microwaves, Optoelectronics and Electromagnetic Applications*, Vol. 18, 399–407, 2019.

[21] Sharma, N. and V. Sharma, "A design of microstrip patch antenna using hybrid fractal slot for wideband applications," *Ain Shams Engineering Journal*, Vol. 9, No. 4, 2491–2497, 2018.

[22] Balanis, C. A., *Antenna Theory*, 2nd ed., John Wiley & Sons, Inc., 1997.

[23] Varshney, A., N. Cholake, and V. Sharma, "Low-cost ELC-UWB fan-shaped antenna using parasitic SRR triplet for ISM band and PCS applications," *International Journal of Electronics Letters*, Vol. 10, No. 4, 391–402, 2022.

[24] Amini, A., H. Oraizi, and M. A. C. zadeh, "Miniaturized UWB log-periodic square fractal antenna," *IEEE Antennas and Wireless Propagation Letters*, Vol. 14, 1322–1325, 2015.

[25] Rao, S. S., S. V. N. Lakshmi, and J. S. Roy, "Design and analysis of microstrip antennas on FR4 substrate for wireless communication," *International Journal of RF and Microwave Computer-Aided Engineering*, Vol. 27, No. 3, 1–9, 2017.

[26] Singh, S., A. Varshney, V. Sharma, I. Elfergani, C. Zebiri, and J. Rodriguez, "A compact off-set edge fed odd-symmetric hybrid fractal slotted antenna for uwb and space applications," *Progress In Electromagnetics Research B*, Vol. 102, 37–60, 2023.

[27] Pozar, D. M., *Microwave Engineering*, 4th ed., 26–30, John Wiley & Sons, Inc., 2012.

[28] Stutzman, W. L. and G. A. Thiele, *Antenna Theory and Design*, John Wiley & Sons, 2012.